Drosophila rae1 is required for male meiosis and spermatogenesis

Silvia Volpi[1], Silvia Bongiorni[2], Fabiana Fabbretti[1], Barbara T. Wakimoto[3] and Giorgio Prantera[1,*]

[1]Department of Ecology and Biology, University of Tuscia, Viterbo, Italy
[2]Department for Innovation in Biological, Agro-Food and Forest Systems, University of Tuscia, Viterbo, Italy
[3]Department of Biology, University of Washington, Seattle, WA 98195-1800, USA

*Author for correspondence (prantera@unitus.it)

Accepted 4 June 2013
Journal of Cell Science 126, 3541–3551

doi: 10.1242/jcs.111328

Summary

Previous studies of RAE1, a conserved WD40 protein, in *Schizosaccharomyces pombe* and mouse revealed a role in mRNA export and cell cycle progression in mitotic cells. Studies of RAE1 in *Drosophila* showed that the protein localizes to the nuclear envelope and is required for progression through the G1 phase of the cell cycle but not RNA export in tissue culture cells. *Drosophila* RAE1 also plays an essential developmental role, as it is required for viability and synaptic growth regulation as a component of an E3 ubiquitin ligase complex. Here we describe characterization of a new *Drosophila rae1* mutant that is viable but results in male sterility. The mutant showed striking defects in primary spermatocyte nuclear integrity, meiotic chromosome condensation, segregation, and spindle morphology. These defects led to a failure to complete meiosis but allowed several aspects of spermatid differentiation to proceed, including axoneme formation and elongation. A GFP–RAE1 fusion protein that rescued most of the cytological defects showed a dynamic localization to the nuclear envelope, chromatin and other structures depending on the stage of spermatogenesis. A role for RAE1 in male meiosis, as well as mitotic cells, was also indicated by the defects induced by expression of *rae1*-RNAi. These studies in *Drosophila* provide the first evidence for an essential meiotic role of RAE1, and thus define RAE1 as a protein required for both meiotic and mitotic cell cycles.

Key words: Meiosis, *rae1*, RNA-export factor, *Drosophila melanogaster*, Mitotic cell cycle regulator

Introduction

The discovery of genes underlying regulation and execution of meiotic events is essential to gain insights into the mechanisms leading to faulty chromosome segregation which contributes to infertility and birth defects in many species including humans. *Drosophila melanogaster* is a particularly amenable organism to study the regulation of meiotic chromosome behavior during gametogenesis. Spermatogenesis in *Drosophila*, and insects in general, has been the favored material for cytological studies because of the large size of male meiocytes. An additional advantage of using *D. melanogaster* is the availability of large collections of mutations disrupting the process. Such mutations have been particularly informative for understanding how entry into meiosis is controlled and how its regulation is coordinated with other complex processes of cellular morphogenesis and differentiation that ultimately lead a functional sperm.

In *Drosophila*, each spermatogonium undergoes four mitotic divisions to generate 16 interconnected primary spermatocytes, which then enter into a long 'growth period' (~90 hours) and become committed to meiosis. The exit from the mitotic cell cycle and the entry into meiosis, is accompanied by a radical change in the gene expression landscape of the primary spermatocyte (Chintapalli et al., 2007). Subsets of newly transcribed genes are required for the meiotic G2/M transition, the meiotic division execution, or to provide regulatory or structural proteins that will be used postmeiotically for spermatid differentiation. Insights into how specific proteins permit the coordination of premeiotic, meiotic and postmeiotic events have been obtained through the study of two classes of genes that differ in their influence on spermatid differentiation. In 'meiotic arrest' class, which includes *can*, *mia* and *aly*, mutant primary spermatocytes do not cross the G2/M border, meiotic divisions do not occur, and unreduced spermatids fail to differentiate, resulting in complete sterility. In the 'twine' class, which includes *twine* and *Dmcdc2*, mutant spermatocytes skip one or both male meiotic divisions, the unreduced spermatids still undergo some aspects of differentiation, but fail in the final steps of sperm individualization. Interestingly studies of the meiotic arrest and twine class genes have identified several proteins that are also involved in mitotic cell cycle, and are either testis-specific paralogs or testis-enriched protein isoforms produced by alternative splicing (reviewed by White-Cooper, 2010). For example, *twine*, encodes a testis-specific Cdc25 paralog, which regulates the activity of the Cdc2-Cyclin B complex and the entry into meiosis (Courtot et al., 1992; White-Cooper et al., 1993), similar to the mitotic role played by its paralog, *string*.

Here we report the characterization of a male sterile recessive mutation, *Z5584* (Wakimoto et al., 2004) and provide additional insight into the regulation of male meiosis and its relationship to regulation of mitosis. We show that *Z5584* results in pleiotropic defects which include disruptions of nuclear integrity in primary spermatocytes, meiotic chromosome missegregation and multiple postmeiotic defects. Molecular analyses show that *Z5584* is a point mutation in the *Drosophila rae1* gene. Ectopic expression of a

rae1-RNAi construct in the germline resulted in male meiotic defects and expression in somatic cells indicated an effect on mitosis. Previous studies have shown that *Schizosaccharomyces pombe* and mouse homologues are essential genes involved in mRNA export and cell cycle progression in mitotic cells (Brown et al., 1995; Whalen et al., 1997; Babu et al., 2003). In *D. melanogaster* tissue culture cells, RAE1 mainly localizes to the nuclear envelope and is required for the progression through the G1 phase of the mitotic cell cycle but not for RNA export (Sitterlin, 2004). Moreover, Tian et al. recently showed that the *D. melanogaster rae1* is an essential gene that regulates neural development as a component of a E3 ubiquitin ligase complex (Tian et al., 2011). Taken together, these new findings and our *in vivo* studies broaden the role of RAE1 in cell regulation and development. In particular, we show that *Drosophila rae1* has a male germ line meiotic function that can be separated by mutation from its somatic function.

Results

Genetic characterization of the *ms(2)Z5584* strain

The *ms(2)Z5584* strain was identified by Wakimoto et al. (Wakimoto et al., 2004) as one of over 1000 lines from the Zuker Collection (Koundakjian et al., 2004) that carried an EMS-treated homozygous viable, recessive male sterile chromosome 2. It was originally classified as defective in meiosis I or II based on the presence of large spermatid nuclei.

Since the *ms(2)Z5584* chromosome was recovered from a heavily mutagenized strain, we used meiotic recombination to map the male sterile phenotype and also obtain derivatives in which the bulk of the chromosome was replaced with unmutagenized sequences. We compared recombinant derivatives which replaced either the left arm or right arm of chromosome 2. One such chromosome named *Rec#57* (al^{-} dp^{-} b^{-} pr^{-} cn^{+} c^{-} *ms(2)Z5584*$^{-}$ px^{+} bw^{-} sp^{+}) resulted in male sterility when homozygous and resulted in the same cytological defects as observed with the original chromosome (data not shown). Conversely, male homozygotes for the reciprocal recombinant (al^{+} dp^{+} b^{+} pr^{+} cn^{-} c^{+} *ms(2)Z5584*$^{+}$ px^{-} bw^{+} sp^{-}) were fertile and exhibited cytologically normal spermatogenesis.

To assess the severity of the *ms(2)Z5584* mutation, we compared the phenotypes of males homozygous for the mutated second chromosome and males hemizygous using the smallest available deletion identified as uncovering *ms(2)Z5584* mutation (see below: mapping results). Both genotypes exhibited complete sterility and coincident meiotic phenotypes. As a whole, these observations suggest that *ms(2)Z5584* second chromosome bears a single severe mutation of a gene acting during, and essential for, spermatogenesis.

The male sterile *ms(2)Z5584* mutation results in failure of spermatogenesis

To determine more precisely which stages of spermatogenesis were affected by the mutation, we first examined testis preparations of wild-type (OreR) and *ms(2)Z5584* homozygous males using phase contrast microscopy. This assay of live, gently squashed tissue permitted a survey of the progression of spermatogenesis. Monitoring the structure and relative sizes of premeiotic, meiotic and postmeiotic nuclei and the spermatid mitochondrial derivative (Nebenkern) provides indicators of normal meiosis and cytokinesis, and the production of motile sperms indicate normal postmeiotic differentiation. As shown in Fig. 1, *ms(2)Z5584* males show prominent defects at multiple stages of spermatogenesis. The earliest defect observed was abnormal nuclear herniations in primary spermatocytes (Fig. 1A,A′). In addition, in contrast to wild-type postmeiotic round spermatids which have uniformly sized nuclei adjacent to similarly sized Nebenkern, the *ms(2)Z5584* spermatids showed wide variations of nuclear and Nebenkern sizes within and among cysts (Fig. 1B,B′). Defects in spermatid differentiation were also observed. Although the mutant produced spermatids with elongated tails, large, round spermatid nuclei failed transition to the needle shaped thin nuclei typical of wild-type spermatids (Fig. 1C,C′). Differentiation arrested prior to spermatid individualization so that the seminal vesicle, which is located at the base of the testis and normally contains motile sperms, was completely lacking mature sperm.

The *ms(2)Z5584* mutation causes defects in meiotic nuclear structure and chromosome behavior, and spermiogenesis

For a higher resolution characterization of the *ms(2)Z5584* defects and to determine consequences on meiosis I versus II, we used fixed testis preparations and immunostaining to examine the distribution of several nuclear, chromosomal and cytoskeletal components at different stages of spermatogenesis. As shown in Fig. 2A, the aberrant nuclear herniations in *ms(2)Z5584* young apolar spermatocytes at S3 stage [staging as referred to by Cenci

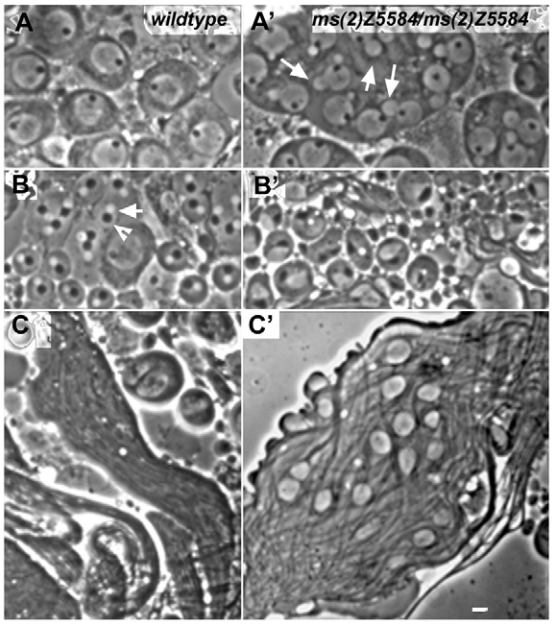

Fig. 1. Defective spermatogenesis in *ms(2)Z5584* males. Phase-contrast microscopy of germ cells from live testes of wild-type (**A–C**) and *ms(2)Z5584* homozygotes (**A′–C′**) show multiple defects in the mutant. Young primary spermatocytes have round uniformly sized, phase light nuclei in the wild type (A) but frequent extensions, or herniations, in the mutant (A′, arrows). Wild-type onion stage spermatids each contain a single phase-light nucleus (B, arrow) and phase-dense Nebenkern (B, arrowhead) of similar size, but the mutant spermatids contain nuclei and Nebenkerns of varying size (B′). In the wild type, spermatid bundles are organized with elongating tails running parallel and thin sperm heads are not distinguishable by phase-contrast microscopy (C) whereas in the mutant, tails are disorganized and nuclei are visible, round and irregularly sized (C′). Scale bar: 10 μm.

et al. (Cenci et al., 1994)] contained chromatin, as revealed by DAPI staining and a distinct lamin signal detected by anti-laminDm0 immunostaining. Hence, these nuclear extensions likely contain an organized lamin network but may result from abnormal chromatin organization or distribution. As previously described by Cenci and colleagues, growth of the primary spermatocyte from early to late stages is accompanied by substantial increase in nuclear size and chromatin movement from the central positions in the nucleus to the nuclear periphery (Cenci et al., 1994). In primary spermatocytes at early prometaphase (M1a stage), the four chromosome pairs occupy distinct nuclear territories, and are detected as DAPI bright chromatin clumps (Fig. 2B). In *ms(2)Z5584* mutants, chromosome pairs appear distinct and occupy separate territories in primary spermatocytes. However, in greater than 90% of prometaphase cells, we observed aberrant condensation, with chromatin clumps showing varying levels of condensed or diffuse DAPI staining. There is also evidence of smaller than normal and variably sized DAPI-positive fragments, suggestive of chromatin fragmentation (Fig. 2C).

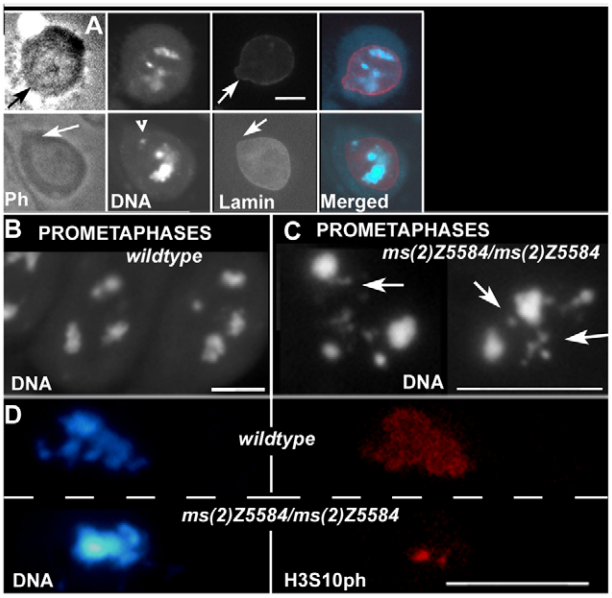

Fig. 2. Aberrant nuclear structures and chromosome condensation in *ms(2)Z5584* primary spermatocytes. (**A**) Nuclear herniation (arrows) in a *ms(2)Z5584* young apolar spermatocyte are surrounded by lamin and may contain chromatin (arrowhead in DNA bottom panel). From left to right: phase contrast (Ph), DAPI, lamin immunostaining and merged image (DAPI in blue, lamin in red). Note that these are fixed preparations and the nuclear area, including herniations, is no longer clearly visible in phase-contrast microscopy and after DAPI staining. (**B**) DAPI staining of wild-type primary spermatocytes at prometaphase (M1a stage) shows three highly condensed chromatin clumps, which are the major bivalents, and a pair of dot-like signals, which are the fourth chromosomes. In contrast, in prometaphase of the *ms(2)Z5584* mutant (**C**) chromatin condensation is aberrant, and there are often variable sized chromatin fragments (arrows). (**D**) Wild-type early (M3 stage) metaphase chromosomes, stained with DAPI (top left panel), congregate at the metaphase plate and exhibit the canonical H3S10ph signal throughout the chromosomes (top right). *ms(2)Z5584* early metaphase chromosomes detected by DAPI staining (bottom left) have the H3S10ph signal only concentrated over small areas of the chromosomes (bottom right). Scale bars: 10 µm.

To further explore the state of chromatin condensation, we immunostained wild-type and mutant testes preparations with an antibody raised against histone H3 phosphorylated at serine 10 (H3S10ph), a marker of meiotic-entry-associated chromosome condensation. As shown in Fig. 2D, the H3S10ph signal is distributed largely throughout the metaphase chromosomes in wild-type primary spermatocytes at M3 stage. In the mutant, H3S10ph is reduced to a small region of the chromatin.

To determine whether the mutation affected meiotic chromosome behavior and spindle organization, we investigated the meiosis progression in the mutant, analyzing stages from metaphase I to telophase I. To recognize the different stages in the mutant, we took advantage of antibodies specific for gamma-tubulin or the centriolar protein SPD-2 (Giansanti et al., 2008), as centrosome markers. In *ms(2)Z5584* cells, all meiotic cysts had at least one abnormal metaphase I or anaphase I figure. Specifically, mutant cysts differed from wild type (Fig. 3A) with metaphases I cells exhibiting poorly organized chromosome configurations and undercondensed chromatin fragments lying outside of the metaphase plates (Fig. 3B), as well as abnormal meiotic spindles with centrosomes mislocated from their typical polar location (Fig. 3C). Anaphases I cells in *ms(2)Z5584* mutants also showed several defects, including lagging chromosomes (Fig. 4A′), chromatin bridges (Fig. 4A″) and unbalanced chromosome segregation to the opposite poles of the dividing cell (Fig. 4A″,A‴).

Chromosome segregation defects were accompanied by anomalies in the spindle structure. Relative to those of wild type, central spindles in the mutant were markedly reduced in microtubule density and were often displaced from the spindle axis (Fig. 4B′). Misoriented microtubules were also visible in telophase spindles (Fig. 4C). Telophases I in the mutant also exhibited abnormal actomyosin ring assembly which is a key component of cytokinesis apparatus together with central spindle. We used an actin-specific Rhodamine–phalloidin fluorescent

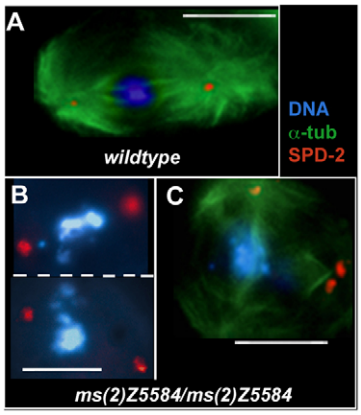

Fig. 3. Metaphase I defects in *ms(2)Z5584* mutants. (**A–C**) Metaphase I cells showing the distributions of DNA (DAPI staining, blue), the meiotic spindle (α-tubulin staining, green) and the centrosomes (SPD-2 staining, red). Note the typical bipolar spindle conformation and the highly condensed bulk of chromatin between the two spindle poles in wild-type meiosis (A). In contrast, in the *ms(2)Z5584* mutant, the chromosome plate is abnormal with fragmented and variably condensed chromatin, some of which lies outside of the plate (B), and with abnormal spindle structure with misplaced centrosomes (C). Note the multipolar organization of the metaphase in C. Scale bars: 10 µm.

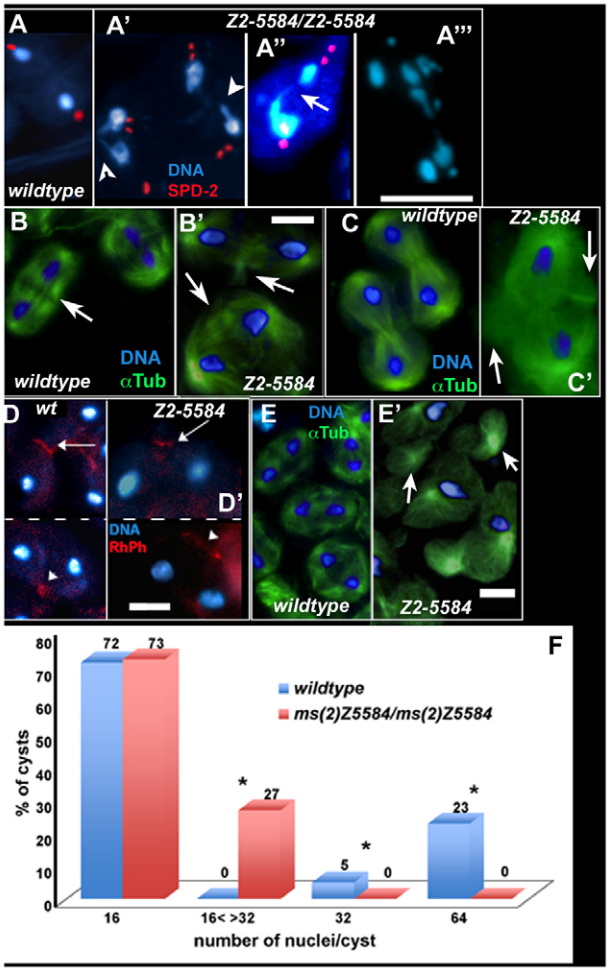

Fig. 4. Anaphase–telophase I defects in *ms(2)Z5584* mutants. (**A–A‴**) Anaphase I cells in wild type (A) and *ms(2)Z5584* mutants (A′–A‴). Note lagging chromosomes (A′, arrowheads), chromatin bridge (A″ arrow; the image is overexposed to show the thin chromatin thread) and unbalanced chromosome segregation to the opposite poles of the cell (A″, A‴) in the mutant. DNA is stained with DAPI (blue) and centrosomes with anti-SPD2 antibody (red). (**B**,**B′**) Spindle defects at anaphase I. Wild-type anaphase spindles are characterized by a dense network of microtubules in the central spindle located between the two segregating chromatin masses (arrow in B) whereas *ms(2)Z5584* anaphase central spindles show a paucity of microtubules, often mislocalized with respect to the spindle axis (arrows in B′). (**C**,**C′**) Aberrantly shaped spindles are visible at telophase I in the mutant (C′). Arrows point to misoriented microtubules. (**D**,**D′**) Rhodamine–phalloidin staining (red; RhPh) was used to visualize actin, a component of the contractile ring. (D) Wild-type early telophase I cells exhibit the actomyosin band at the midzone (arrow), which progressively constricts to a small ring (arrowhead). (D′) In *ms(2)Z5584* mutants at telophase I the actomyosin ring either assembles properly and constricts (arrow) or assembles but does not constrict (arrowhead). (**E**,**E′**) Meiosis I cysts in wild type (E) and *ms(2)Z5584* mutants (E′). Note the presence of asters devoid of chromatin in the mutant (arrows in E′). Scale bars: 10 μm. (**F**) Histogram comparing cyst composition in wild type and *ms(2)Z5584* mutants. The asterisks denote statistically significant differences between the wild type and *ms(2)Z5584* mutant (χ^2-test).

staining to detect the actomyosin ring, which appears as a thin band at the midzone in wild-type early telophase, then as a ring-shaped structure between the late telophase nuclei (Fig. 4D). In the mutant, the actomyosin ring showed variable behavior, being properly formed and constricted in some cells (Fig. 4D′, arrow) and unconstricted (Fig. 4D′, arrowhead) or absent (not shown) in other cells. Abnormalities in chromosome segregation also showed variability at cytological level. Meiosis I cysts showed occasional cells with spindles that were devoid of chromatin (Fig. 4E′). Strikingly, we did not detect meiosis II figures in *ms(2)Z5584* mutant testes.

These findings prompted us to undertake a statistical analysis of the occurrence of cysts containing 16 primary spermatocytes, 32 secondary spermatocytes or 64 spermatids in wild-type and *ms(2)Z5584* homozygotes. As expected, wild-type cysts containing 16, 32 or 64 nuclei were observed but cysts with intermediate numbers were not observed. In contrast, *ms(2)Z5584* testes had cysts with 16 nuclei and cysts with a number of nuclei ranging between 16 and 32; no cysts with 32 or 64 nuclei were observed (Fig. 4F). These data indicate that mutant meiocytes routinely fail prior to the completion of Meiosis I and do not progress to Meiosis II.

Despite the multiple meiotic alterations described above, phase-contrast microscopy of *ms(2)Z5584* mutant showed that some aspects of cellular differentiation proceed (Fig. 1B′,C′).

We used immunocytological analysis to monitor centriolar, nuclear, and actin distributions in later stages of spermatogenesis and found frequent abnormalities in differentiation. These defects included two mislocalized centrioles instead of a single normally positioned centriole in onion stage spermatids (Fig. 5A,A′), improper nuclear shaping and cyst polarization in elongating

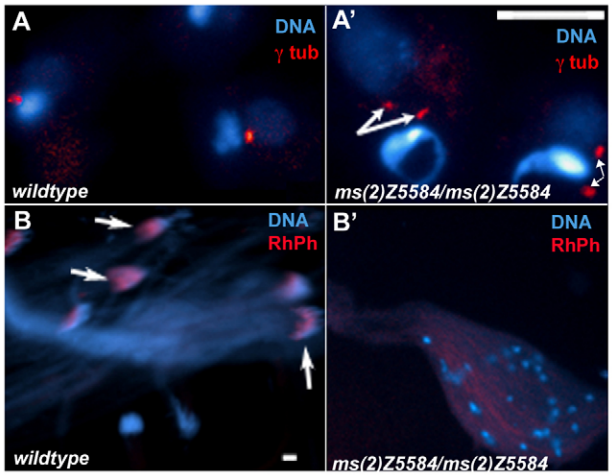

Fig. 5. Aberrant spermiogenesis in *ms(2)Z5584* spermatids. (**A**) Two wild-type onion stage spermatids show a single centriole, identified by γ-tubulin immunostaining (red), often localized between the nucleus (DAPI brightly stained mass) and the Nebenkern (DAPI weakly stained mass). In the mutant (**A′**), spermatids have two mispositioned centrioles per nucleus (arrows). (**B**) Wild-type DAPI-stained spermatid bundles with needle-shaped nuclei that are polarized to the same end of the bundle. Rhodamine–phalloidin fluorescence (red) identifies the actin-based cones, representing individualization complexes (ICs), which assemble on each of the 64 spermatid nuclei of the bundle and move synchronously along the tail toward the end. In this image, they are visible beneath the heads of each spermatid (arrows). (**B′**) *ms(2)Z5584* spermatid bundles are characterized by the presence of round nuclei, dispersed along the bundle. Note the absence of localized Rhodamine–phalloidin fluorescence, which demonstrates the failure of IC assembly in the mutant. Scale bars: 10 μm.

sperm bundles, and failure of the assembly of the actin-rich individualization complexes (Fig. 5B,B′), preventing the complete differentiation and release of mature gametes from the testis.

In conclusion, the *ms(2)Z5584* mutation resulted in pleiotropic effects evident throughout spermatogenesis. The earliest visible defect observed was nuclear protrusions in growing primary spermatocyte and abnormalities in prometaphase chromosome condensation. Meiosis I chromosome segregation and spindle morphologies were also defective and the likely consequence of these may be a failure to complete meiosis I. One or more of the premeiotic or meiosis I defects may lead to the multiple postmeiotic anomalies.

ms(2)Z5584 is a mutation in the *rae1* gene

To identify the *ms(2)Z5584* gene, we first mapped the mutation using meiotic recombination to the distal right arm of chromosome 2, then tested a series of 2R deficiency chromosomes (see Materials and Methods) for their ability to complement the *ms(2)Z5584* male sterility. Two overlapping deletions, *Df(2R)ED3923* and *Df(2R)BSC424*, refined the localization to within the 57F6 cytogenetic interval and a 40.592 kb region defined by the proximal breakpoints of the two deficiencies. The most recent release of the Drosophila Genome Project (McQuilton et al., 2012) annotated 17 putative genes within this region, of which 11 had insertions that disrupted the gene. We tested these insertions in combination with *ms(2)Z5584* and found that all complemented *ms(2)Z5584* resulting in fertile males and suggesting that the corresponding genes were unlikely candidate genes. Four of the remaining genes, namely *CG30284*, *rae1*, *CG15676* and *NC2alpha*, were selected as genes of higher interest on the basis of previously reported expression in the testis and/or a predicted molecular function consistent with the *ms(2)Z5584* phenotype. Sequencing these four genes in the *ms(2)Z5584* strain identified a point mutation in the open reading frame of only the *rae1* gene. This mutation resulted in a G/C to A/T transition which was predicted to result in a glycine (G) to aspartic acid (D) substitution, at position 129 in the predicted 346 amino acid RAE1 protein.

Previous studies have shown that RAE1 is a WD40-repeat-containing protein with orthologs present in a wide variety of eukaryotes, including yeast, protozoans, plants and animals (Brown et al., 1995; Murphy et al., 1996; Bharathi et al., 1997; Pritchard et al., 1999; Sabri and Visa, 2000; Sitterlin, 2004; Lee et al., 2009). Amino acid sequence alignment of RAE1 orthologs using CLUSTALW shows that the *Drosophila* protein has extensive sequence identity with other family members (supplementary material Fig. S1). The functional importance of glycine 129 is suggested by its evolutionary conservation in RAE1 proteins from yeast to humans, and its location within a highly conserved 12 amino acid domain in the third putative WD40 repeat (supplementary material Fig. S1). Taken together, these studies warrant the designation of *ms(2)Z5584* as $rae1^{Z5584}$.

$rae1^{Z5584}$ is the first and thus far only reported *Drosophila rae1* mutation with a documented role in meiosis and spermatogenesis. The availability of strains to conditionally express double stranded *rae1* RNA (RNAi) in the testis allowed us to test whether RNAi-induced phenotypes were similar to those observed in $rae1^{Z5584}$ homozygotes. To this end, *rae1* dsRNA was expressed under the control of Gal4 promoter whose expression is regulated by a germline-specific Gal4 driver, *BamG4UASDicer2* (see Materials and Methods). This resulted in male sterility with testes defects identical to those observed in $rae1^{Z5584}$ homozygotes (Fig. 6). In particular, nuclear herniations in primary spermatocytes were clearly apparent (Fig. 6A) while meiotic division defects both *in vivo* (Fig. 6B) and in fixed preparations (Fig. 6D,E) strongly resembled those of $rae1^{Z5584}$ homozygotes (compare irregular metaphase plates in Fig. 6E,E′ and those in Fig. 3B; compare lagging chromosomes in Fig. 6D and those in Fig. 4A′–A‴). These results are consistent with our gene assignment and our conclusion of $rae1^{Z5584}$ requirement for normal nuclear organization in primary spermatocytes and completion of Meiosis I. In *D. melanogaster*, a Rae1 homolog, CG12782, exists and maps on the second chromosome right arm. We tested two deficiencies that uncovered *CG12782*, each in trans-heterozygous condition with $rae1^{Z5584}$, but we did not detect an effect on male fertility. This does not exclude the possibility of interactions between the two homolog genes, that might be revealed in more sensitive assays. We did note that the highly conserved RAE Gly 129 which our mutation shows is

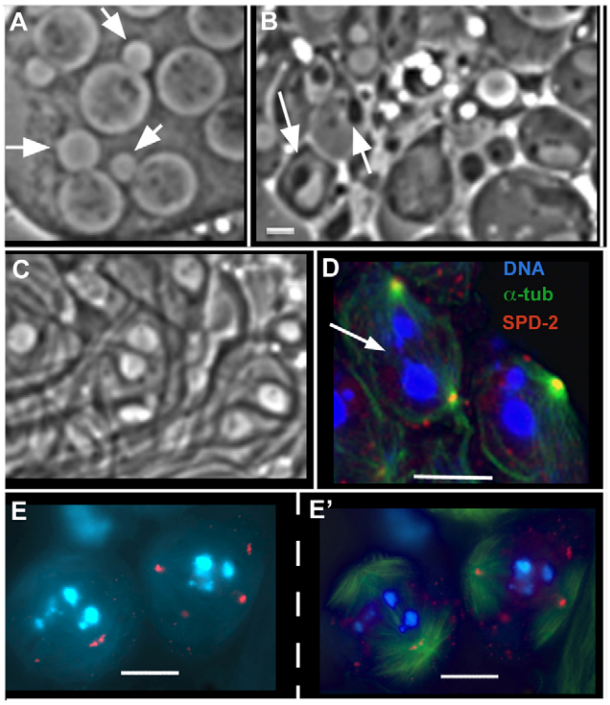

Fig. 6. Testes defects after the expression of *rae1* dsRNA under the control of a testis-specific Gal4 driver. (**A–C**) Phase-contrast microscopy of live testes dissected from *rae1* RNAi-treated males showing identical defects to those observed in $rae1^{Z5584}$ homozygotes: (A) young primary spermatocytes with herniations (arrows); (B) onion stage spermatids with nuclei and Nebenkern of varying sizes (arrows); and (C) spermatid bundle with scattered, round and irregularly sized nuclei. (**D–E**) Metaphase I and anaphase I cells showing the distributions of DNA (DAPI staining, blue), meiotic spindles (α–tubulin staining, green) and centrosome (SPD-2 staining, red). (D) Confocal microscope image of two adjacent early anaphases showing lagging chromosomes and unbalanced chromosome segregation to the opposite poles as it was observed in *ms(2)Z5584* homozygotes (compare Fig. 6D and Fig. 4A′–A‴). (E,E′) The same metaphase plates showing (E′) or not showing (E) the meiotic spindle. Note the undercondensed chromatin fragments lying outside the metaphase plates, which strongly resemble those of *ms(2)Z5584* mutants (compare Fig. 6E and Fig. 3B). Scale bars: 10 μm.

critical for male meiosis, is not present in the CG12782 predicted protein.

Localization and activity of a GFP–RAE1 fusion protein in the male germline

To assess the localization of RAE1 in meiotic cells, we took advantage of a *D. melanogaster* transgenic strain carrying a *UAS-GFP-rae1* transgene (Tian et al., 2011). To drive the transgene expression in the testis, we combined it with the germline-specific *BamG4UASDicer2* and the ubiquitous *tubulinGal4* drivers. Both the drivers gave the same GFP–RAE1 distribution pattern in meiotic cells, but the Bam Gal4 driver did not yield a detectable GFP signal in pre and postmeiotic cells. Therefore, the ensuing description refers to results obtained with the constitutive *tubulinGal4* driver. In intact testes, the fusion protein GFP signal was apparent in all the cellular stages from spermatogonia to sperms. In spermatogonia (not shown) and in young primary spermatocytes (S1 to S4 stages) (Cenci et al., 1994) GFP–RAE1 appeared as a distinct rim at the nuclear envelope (Fig. 7A), similar to that observed in *D. melanogaster* SL2 culture cells transfected with a HA-tagged RAE1 (Sitterlin, 2004). In S1–S4 spermatocytes, the chromatin appeared devoid of GFP–RAE1. As the primary spermatocytes progressed toward late prophase stages, GFP–RAE1 localized with the three chromatin clumps (Fig. 7B, arrows) and cytoplasmic GFP–RAE1 was also apparent (Fig. 7B). In anaphase I and telophase I, the GFP–RAE1 coincided with segregating chromatin and with the DAPI-positive mitochondria that localized between the two daughter nuclei (Fig. 7C). In postmeiotic onion stage spermatids, GFP–RAE1 appeared predominantly associated with Nebenkern (Fig. 7D), with little or no nuclear signal detected. In mature sperms, GFP–RAE1 appeared associated with both nuclei and tails (Fig. 7E).

To assess if the GFP–RAE1 protein could substitute for the wild-type RAE1 we challenged the chimeric construct to rescue the $rae1^{Z5584}$ homozygous male sterility (see supplementary material Fig. S2 for details). We found that the *rae1* transgene was unable to restore the male fertility. However, cytological analysis of the *GFP-rae1*-expressing, mutant males revealed partial rescue of at least some of the meiotic defects. In particular, young primary spermatocytes appeared normal and lacked the characteristic nuclear herniations that were commonly

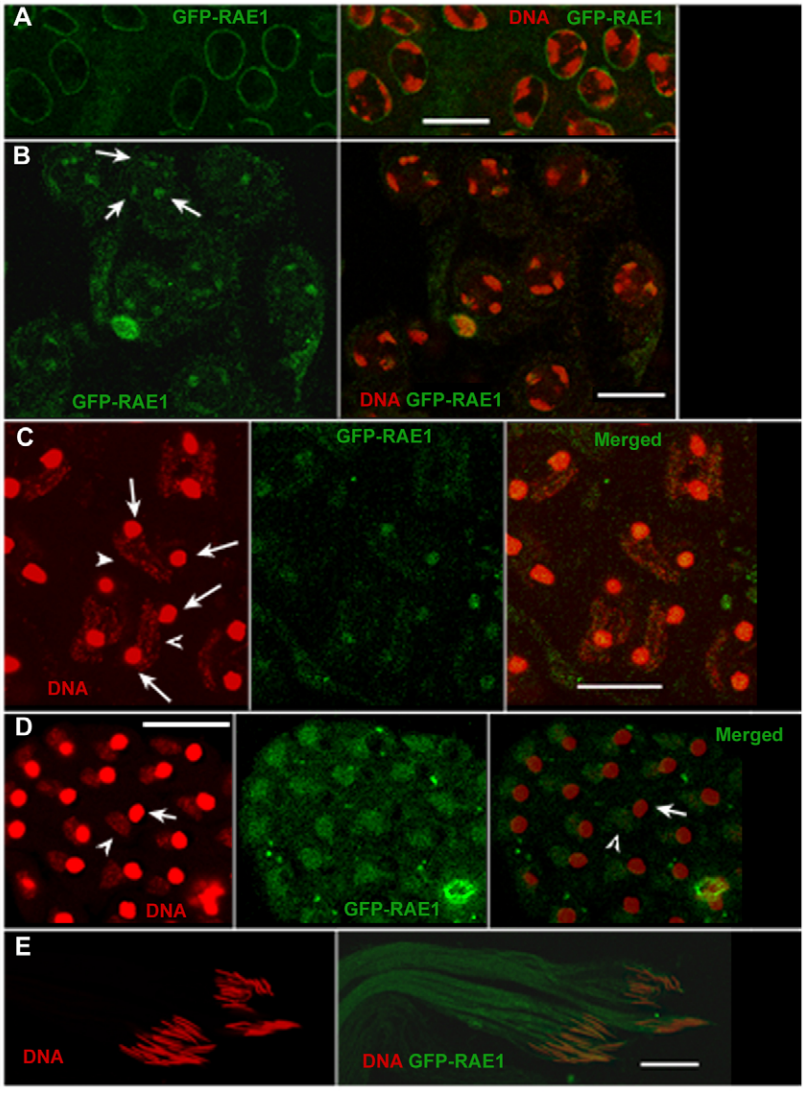

Fig. 7. Confocal analysis of the localization of GFP–RAE1 in wild-type testes. In all the images, DNA (DAPI) is in red and GFP–RAE1 in green. (**A**) In young primary spermatocytes, GFP–RAE1 has a perinuclear distribution. (**B**) In late meiotic prophase cells, GFP–RAE1 signal is nuclear, where it coincides with the three major chromatin clumps (arrows) and is also distributed over the cytoplasm with a punctate pattern. (**C**) In anaphase/telophase I cells, GFP–RAE1 is associated with the nuclear DNA (arrows) and mitochondria (arrowheads). (**D**) In onion stage spermatids, GFP–RAE1 signal is mainly associated with the Nebenkern (arrowheads), whereas a nuclear signal is absent (arrows). (**E**) The GFP–RAE1 signal marks both heads and tails of mature sperm. Scale bars: 20 μm.

Table 1. Mitotic parameters of *Ore-R*, *rae1*^{Z5584} mutant homozygous, hemizygous and *rae1 RNAi/wor-Gal4* larval brains

Genotype	Optical fields	Mitotic figures	Mitotic index[a]	Anaphases (%)	Defective anaphases[c] (%)
Ore-R	1507	1224	0.81	8	1
rae1Z5584/rae1Z5584	805	662	0.82	4[b]	NA
rae1Z5584/Df(2R)ED3923	911	865	0.95[b]	1[b]	NA
rae1 dsRNA/wor-Gal4	362	556	1.54[b]	8	70[b]

[a]The mitotic index is the number of mitotic figures per optical field (see Materials and Methods).
[b]Significant values ($P<0.01$) calculated by χ^2-test with respect to control *Ore-R*.
[c]Defective anaphase figures consist of lagging chromosomes, chromatin bridges and uneven chromosome segregation. NA, not assessed.

observed in the mutant (supplementary material Fig. S3A). Moreover, chromosome segregation appeared normal at metaphase I (data not shown) and onion stage spermatids exhibited the 1:1 nuclear to Nebenkern ratio typical of wild-type cells, although some nuclei and Nebenkerns appeared to have irregular shapes (supplementary material Fig. S3B,C). Spermatid elongation was evident but cysts showed nuclear misalignment typical of the *rae1*^{Z5584}. However, nuclear morphology appeared to be intermediate between the round uncondensed spermatid nuclei of the mutant and the highly condensed sperm head of normal sperm (supplementary material Fig. S3D).

To determine the extent to which GFP–RAE1 supported the completion of the meiotic divisions, we asked whether males that were homozygous for *rae1*^{Z5584} and expressing the GFP–RAE1 transgene had cysts containing 16, 32, 64 or an intermediate number of germ cells. We performed nuclear counts within intact cysts of two males. In contrast to *rae1*^{Z5584} homozygotes (Fig. 4F), the transgenic males showed some 32 and 64 cell cysts, indicating that GFP–RAE1 is capable of supporting the progression and completion of meiosis I and II, although variably so. The apparent absence of motile sperm in these males show expression of the GFP–RAE1 is not able to rescue postmeiotic differentiation.

Assessment of the role of *rae1* in mitosis

To investigate a possible role of *Drosophila rae1* in mitosis, we asked if the *rae1*^{Z5584} mutation affected the mitotic parameters of neuroblasts in the central nervous system (CNS) in third instar larvae. We determined a mitotic index for this tissue for *rae1*$^{+}$ control (*Ore-R*) larvae (see Materials and Methods) and compared this to indices for *rae1*^{Z5584} homozygotes and hemizygotes. We also counted the number of anaphase configurations for each genotype. As summarized in Table 1, *rae1*^{Z5584} hemizygotes showed a statistically significant higher mitotic index and lower frequency of anaphases relative to the control. *rae1*^{Z5584} homozygotes show instead only a decrease of anaphase figures. In this context it should be noted that neither the *rae1*^{Z5584} homozygotes nor the hemizygotes showed reduced viability.

As a complementary approach, we expressed *rae1* RNAi under the control of the neuroblast-specific driver *wor*-GAL4 (Cabernard and Doe, 2009), and examined the consequences. The mitotic index in the CNS of third instar larvae expressing the *rae1* RNAi was higher than controls (Table 1) but the frequency of anaphase configurations was not statistically different from controls. However, the majority of anaphase figures (70%) appeared defective in *rae1* interfered larval brains (Table 1). The defects included lagging chromosomes, chromatin bridges and uneven chromosome segregation (not shown). Interestingly, in colchicine-treated, Rae1-depleted larval brains, metaphase chromosomes appeared undercondensed (Fig. 8). Thus, reduction of RAE1 induces a detectable effect on the mitotic cell cycle and mitotic chromosome morphology. The developmental consequences of these defects are not known, but we note that we did not detect an effect on viability.

Discussion

Our discovery that a male sterile mutation, *ms(2)Z5584*, resides in the *D. melanogaster* ortholog of the *rae1* gene has implications for understanding the function of the RAE1 protein. The protein is a WD40-repeat β propeller protein, with four evolutionarily conserved WD repeats. A wide variety of functions have been identified for the members of the WD40-repeat protein superfamily, leading to the proposal the common property is the ability to assemble multiple proteins in large macromolecules (Neer et al., 1994). *rae1* is evolutionarily highly conserved from yeast to mammals (Reddy et al., 2008), and it was first identified in the fission yeast *Schizosaccharomyces pombe* as a nucleoporin involved in poly(A)$^{+}$ mRNA export and cell cycle progression (Brown et al., 1995; Whalen et al., 1997). The interaction between RAE1 and the nucleoporin NUP98 was demonstrated in human cells (Pritchard et al., 1999) and aberrant poly(A)$^{+}$ mRNA accumulation in the nucleus was documented in *rae1* (*gle2*)

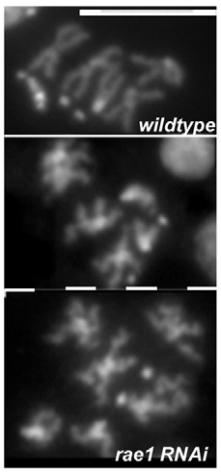

Fig. 8. Effect of *rae1* dsRNA on mitotic chromosome morphology. Comparison of chromosome morphology in neuroblasts from wild-type larvae and larvae expressing *rae1* RNAi. Wild-type neuroblasts (top panel) show uniform condensation of chromosomes after DAPI staining, with heterochromatic regions appearing relatively bright. Expression of rae1 RNAi resulted in chromatin undercondensation in metaphase chromosomes (bottom panels). Scale bar: 10 μm.

mutants in *Saccharomyces cerevisiae* (Murphy et al., 1996). However, subsequent studies revealed pleiotropic effects of *rae1* in various organisms, indicating a broader function for the protein in mitosis. For example, in human cells, RAE1 interacts with the mitotic checkpoint protein BUB1 (Wang et al., 2001) and with the mitotic apparatus protein NUMA (Wong et al., 2006), suggesting a role for *rae1* as mitotic regulator. Moreover, a direct binding of RAE1 to securin, blocking its degradation and thus regulating the metaphase to anaphase transition was reported (Jeganathan et al., 2005; Jeganathan et al., 2006).

In *D. melanogaster*, *rae1* was investigated in SL2 culture cells by dsRNA interference by Sitterlin who showed that this resulted in cell cycle arrest at G1/S transition, but neither mitotic anomalies nor mRNA accumulation in the nucleus were observed (Sitterlin, 2004). Very recently, Tian et al. clearly demonstrated that in *Drosophila*, RAE1 is involved in the regulation of neural development (Tian et al., 2011). Using a combination of genetic and biochemical analyses, these authors elegantly showed that RAE1 positively regulates the abundance of the E3 ubiquitin ligase Highwire, which in turn restrains the growth of synapses at the neuromuscular junctions (Tian et al., 2011).

Our cytological and molecular characterization of the *ms(2)Z5584* mutation provides the first evidence of an *in vivo* role of *rae1* in the meiotic cell cycle. The specific mutation we discovered is a glycine to aspartic acid substitution. This glycine is an invariant amino acid within a 12 amino acid domain which is highly conserved in RAE1 hortologs in a wide range of species from yeast to humans. By mobilizing a transposable P-element in *D. melanogaster*, Tian et al. obtained two *rae1* imprecise excision alleles which were homozygous lethal at the second instar larval stage (Tian et al., 2011). In the light of these results and the lethality of *rae1* null mice (Babu et al., 2003), and given the well-established role of *rae1* in mitosis in many species, it is rather surprising that $rae1^{Z5584}$ homozygous flies are fully viable with no effect on the mitotic index of larval neuroblasts. Hemizygous individuals, however, even though fully viable, show an increased mitotic index in the CNS. We also observed a reduction in the number of anaphase configuration which is indicative of a mitotic delay. In this context, it is notable that *rae1* haploinsufficiency produces mitotic anomalies in mammals (Babu et al., 2003). In accordance with the results in other organisms, the CNS-specific expression of *rae1* dsRNA produced mitotic anomalies in neuroblast cells. Because the main effect of decreased RAE1 in dividing cells is cell cycle arrest at the G1/S transition, the apparent absence of mitotic anomalies in *D. melanogaster* SL2 culture cells following *rae1* dsRNA interference (Sitterlin, 2004) might have been due to the fact that successfully interfered cells arrest prior to the G1/M transition so do not enter mitosis. Taken together, studies using *Drosophila* and those using other organisms provide a consistent view of RAE1 as a conserved mitotic cell cycle regulator (Brown et al., 1995; Whalen et al., 1997; Wang et al., 2001; Wong et al., 2006; Sitterlin, 2004; Jeganathan et al., 2006). Our studies of $rae1^{Z5584}$ are the first to suggest a meiotic role. We do not yet know if the meiotic role of RAE1 is limited to *Drosophila* males or if it is also important for *Drosophila* females and meiosis in other organisms.

The multiple defects we observed in *ms(2)Z5584* mutant males affected both early meiotic stages and late spermiogenesis. The earliest defects we observed in mutant primary spermatocytes are nuclear envelope herniations, which resemble those found in *gle-1* (the *rae1* ortholog) mutants in *S. cerevisiae* (Murphy et al., 1996). This observation is consistent with a localization of RAE1 to the nuclear envelope in wild-type spermatogonia and primary spermatocytes as suggested by our studies of the GFP–RAE1 fusion protein and with the pattern of HA-tagged RAE1 in *D. melanogaster* SL2 culture cells (Sitterlin, 2004). Primary spermatocytes lacking RAE1 showed nuclear herniations. Notably the nuclear lamin appeared continuous even in these herniations. Most consistently we observed that the mutant showed defective meiotic chromatin condensation which accompanied by the nearly total loss of the chromosome condensation marker, histone H3 serine 10 phosphorylation. We may thus hypothesize that RAE1 is necessary at nuclear envelope in primary spermatocytes to direct meiotic chromatin organization and condensation, whose alteration may explain the ensuing meiotic anomalies. In this context it is notable that the defective chromosome condensation is also a distinctive trait of *rae1*-interfered somatic cells. Interestingly, mutations in *dTopors*, the *Drosophila* homolog of the mammalian dual ubiquitin/small ubiquitin-related modifier (SUMO) ligase Topors result in male sterility and spermatocyte nuclear membrane blebbing similar to *ms(2)Z5584* mutants. Remarkably, *dTopors* mutants also exhibit meiosis I defects, such as chromosome missegregation and anaphase I bridges (Matsui et al., 2011). These results suggest that *rae1* and *dTopors* genes may be involved in the same pathway. A demonstration of a genetic and physical interaction of RAE1 and dTOPORS in male germ cells would be consistent with results of Tian et al. showing that RAE1 physically interacts with the E3 ubiquitin ligase Highwire in the CNS (Tian et al., 2011). The analysis of GFP–tagged RAE1 distribution in wild-type meiosis I cells indicated co-localization of RAE1 with chromatin starting from late prophase primary spermatocytes until ana/telophase I nuclei, thus suggesting that the role of RAE1 in chromatin condensation may be more direct. In meiosis, bivalents need to reach a correct condensation state during late G2/prophase I to ensure a faithful chromosome partitioning to daughter cells, through the resolution of homologous associations, necessary to prevent chromatin bridges (Hartl et al., 2008). Hence, defective chromosome condensation could explain the lagging chromosomes and anaphase bridges, culminating in an uneven chromosome segregation to the opposite cell poles of the first meiotic division. Concomitantly, we detected also several defects affecting meiotic spindle and centrosomes. Metaphase I figures are reminiscent of the abnormal, multipolar spindles associated with multiple pericentrin foci, which cause defects of mitotic chromosome alignment and segregation in *rae1* dsRNA-treated HeLa cells (Blower et al., 2005). The involvement of RAE1 in mitotic spindle assembly has been previously proposed by the identification of RAE1 association with NuMA (nuclear mitotic apparatus) (Wong et al., 2006). This complex associates with dynein at spindle poles, and is crucial for spindle bipolarity in HeLa cells, where the interaction between RAE1 and the cohesin subunit SMC1 was also reported, which is required for proper spindle formation (Wong et al., 2006; Nakano et al., 2010; Wong, 2010). Moreover, a disorganization of tubulin and actin networks was also documented in *S. pombe rae1-1* mutant cells (Brown et al., 1995). Furthermore, in *ms(2)Z5584* mutant males we also observed ana/telophase I central spindle anomalies. The mitochondria are uniformly distributed within the cytoplasm of late prophase I cells and associate with the central spindle at

anaphase (Fuller, 1993; Cenci et al., 1994). Our cytological preparations were particularly helpful to reveal the behavior and distribution of mitochondria by DAPI staining. In this context it is remarkable that in wild type, GFP-tagged RAE1 localized with mitochondria distributed between ana/telophase I daughter nuclei where the central spindle is assembled. *ms(2)Z5584* male meiosis thus showed both karyokinesis and cytokinesis defects that account for the presence of spermatids at onion stage with nuclei and Nebenkern of variable size. *ms(2)Z5584* non-reduced spermatid exhibited two mispositioned centrioles as opposite to wild-type spermatids where a single centriole, juxtaposed to the nucleus, will become the basal body. This latter will then play a central role in nuclear shaping and cyst polarization (Fuller, 1993). Consistently with this scenario, in *ms(2)Z5584* late spermatids the nuclear transition from a rounded to a needle-like shape is impaired, and cyst polarization does not occur. Nevertheless, in *ms(2)Z5584* mutants, unreduced spermatids that exit from the defective meiotic divisions proceed to accomplish some differentiation including axoneme assembly and elongation. This behavior is quite similar to that of the Twine Class of male sterile mutants. The genes of this class, such as *Dmcdc2* and *twine* itself, have been shown to preside the entry into meiosis, regulating the activity of Cdc2–Cyclin B complex, underlying M-phase progression. Their null mutants skip both meiotic divisions; nonetheless they initiate and enact some steps of differentiation (Alphey et al., 1992; Courtot et al., 1992; White-Cooper et al., 1993; Maines and Wasserman, 1999; Sigrist et al., 1995). *ms(2)Z5584* mutants enter first meiotic division, as testified by the presence of, albeit irregular, metaphase I and anaphase I figures. This indicates that *rae1* acts downstream of the meiotic entry. In $rae1^{Z5584}$ mutants, secondary spermatocytes are formed with unbalanced chromosome distribution and even devoid of chromosomes. Nevertheless, mutant secondary spermatocytes fail to execute the second meiotic division. This is rather surprising because of the lack of an efficacious spindle checkpoint in *Drosophila* spermatocytes (Basu et al., 1999; Rebollo et al., 2004), and the behavior of *fusolo* and *solofuso* mutants, in which secondary spermatocytes, although devoid of chromatin, execute a second meiotic division (Bucciarelli et al., 2003). This would imply that RAE1 plays a role in the second meiotic division execution too, as suggested also by the colocalization of RAE1 with the ana/telophase I chromatin and with mitochondria at the central spindle in wild type, that indicates an accurate partitioning between the two secondary spermatocytes.

The persistence of GFP-tagged RAE1 in wild-type postmeiotic cells may reflect a role for RAE1 in spermatid differentiation, consistent with the observed defects of $rae1^{Z5584}$ homozygotes at these stages. Interestingly, we noted a difference between the fully round spermatid nuclear phenotype in the mutant and the partially condensed spermatid nuclei induced with GFP–RAE1 expression. This may reflect partial rescue and a direct role of RAE1 in spermatid chromatin condensation. We do not know if the inability to achieve complete condensation is due to abnormal function of the chimeric protein or to its abnormal regulation since the construct did not use the *rae1* promoter. Regardless, the failure of spermatid with abnormal chromatin condensation to initiate individualization is not surprising since this is a common mutant phenotype (Wakimoto et al., 2004) and it accounts for the inability of the *GFP-rae1* transgene to restore fertility to $rae1^{Z558}$ mutants.

The documented interaction of RAE1 with a E3 ubiquitin ligase (Tian et al., 2011) may account for an indirect role of RAE1 on chromatin dynamics via the ubiquitin pathway. This interaction may also account for the pleiotropic defects seen in *ms(2)Z5584* spermatogenesis. The proposed involvement of RAE1 with nucleoporins has been strengthened in recent years, with its inclusion in a wide variety of molecular networks, embracing processes that also include chromosome condensation, kinetochore assembly and spindle formation during mitosis (Nakano et al., 2010). One possibility is that there is a novel and unexpected meiosis-specific function of RAE1 as a nucleoporin. We can hypothesize a model in which NPC proteins such as RAE1 are required at nuclear pores in meiotic prophase for docking chromosomes to the nuclear envelope and promoting proper chromosome condensation, as essential prerequisite for a correct chromosome segregation. Accordingly, *rae1* loss of function would cause both the chromosome condensation and segregation defects which are distinctive of *ms(2)Z5584* mutant 1st meiotic division. Moreover, the *ms(2)Z5584* mutant meiotic spindle organization and behavior is also damaged, in agreement with the reported RAE1 role in mitosis (Wong et al., 2006; Nakano et al., 2010; Wong, 2010). The severe postmeiotic defects of *ms(2)Z5584* may be the results of the lack of an efficacious spindle checkpoint in *Drosophila* spermatocytes, able to arrest the system in case of meiotic anomalies (Basu et al., 1999; Rebollo et al., 2004), and of a possible role for RAE1 in postmeiotic spermatid differentiation stages. This is exemplified by the pleiotropic effects of *Drosophila* meiotic mutants like, for example, *asunder* (Anderson et al., 2009) and *larp* (Ichihara et al., 2007).

In conclusion, our data strongly indicate an unanticipated involvement of RAE1 in meiosis and a requirement for RAE1 function for postmeiotic differentiation of the male germ line in *Drosophila*. The possibility of a conserved function for RAE1 in meiosis and male fertility provides new avenues for studying how the protein acts at the cellular and mechanistic levels in two different types of cell division.

Materials and Methods

Fly strains and gene mapping

The *ms(2)Z5584* line was provided by Koundakjian et al. (Koundakjian et al., 2004). It was identified from the Zuker collection in a screen for ethyl methanesulfonate (EMS)-induced recessive male sterile mutations and classified as defective in male meiosis by Wakimoto et al. (Wakimoto et al., 2004). The mutation was induced on a second chromosome marked with *cn* and *bw*, kept in stock with the balancer *CyO*, *Cy* cn^2. We used the following GAL4 driver stocks: *BamG4UASDicer* (kindly provided by M. Fuller, Stanford University); and *w; wor-Gal4,UAS-cherry::Zeus,w+/CyO;Dr/TM6B,Tb,Hu,e* (kindly provided by C. Doe, University of Oregon); and *tubulinGal4/TM6B;Sb*. The *UAS-GFP-rae1*/TM6B;*Sb* line was kindly provided by Chunlai Wu (Neuroscience Center, Louisiana State University, Health Sciences Center). The *rae1* RNA-interfered line was obtained from the VDRC (Dietzl et al., 2007). All other stocks were obtained from the BDSC at Indiana University.

Flies were raised on standard Drosophila medium at 25℃, except for crosses involving *BamG4UASDicer* which required growth at 29℃. For assays of male fertility, crosses generally involved one to three males and three to five females in a single cross. Those that yielded no progeny in two separate trials were classified sterile.

The *ms(2)Z5584* male sterility was mapped by meiotic recombination relative to the recessive *al*, *dp*, *b*, *pr*, *c*, *px* and *sp* markers and tests involving 100 recombinant chromosomes indicated a map position of ~96.2 m.u. on the right arm of chromosome 2. Two recombinant chromosomes were maintained in stocks over the *CyO*, or *T(2;3)Cy; Tb* balancers for use in subsequent experiments. One chromosome was $al^- dp^- b^- pr^- cn^+ c^- px^+ bw^- sp^+$, resulted in sterility and was denoted *Rec#57 ms(2)Z5584*. A reciprocally marked chromosome $al^+ dp^+ b^+ pr^+ cn^- c^+ s^+ px^- bw^+ sp^-$ resulted in fertility. These chromosomes were tested in homozygotes to verify that the observed spermatogenesis defects were due to solely to the region to which the male sterility mapped. Mapping with deficiency

chromosomes allowed us to refine the localization of *ms(2)Z5584* to the 57F6 cytogenetic interval, within the 40.592 kb region defined by the proximal breakpoints of *Df(2R)ED3923* and *Df(2R)BSC424*. Complementation crosses were also performed between *ms(2)Z5584/CyO* and strains that contained insertions proposed to affect the following genes located in this region: *CG10082*, *CG10320*, *pirk*, *CG42362*, *CG42379/CG42380/CG42381/CG9865*, *CG30263*, *CG10306* and *Tbp*. In all of cases, the insertion mutation complemented the *ms(2)Z5584* sterility.

Cytological analyses of spermatogenesis

Testes from *ms(2)Z5584* mutant males or control males (OreR) were dissected within 1 day of eclosion in testis isolation buffer, TIB (183 mM KCl, 47 mM NaCl, 10 mM Tris pH 6.8). For observations of unfixed samples, testes were placed in 10 µl of buffer on a slide, overlaid with a coverslip, and observed using phase contrast optics on an Zeiss Axiophot microscope. To preserve whole cysts, testes were placed on a slide under a siliconized coverslip, the slide frozen in liquid nitrogen, then the coverslip removed with a razor blade, before the tissue was dehydrated in cold ethanol, then fixed for 7 minutes in 2% paraformaldehyde in 1×phosphate-buffered saline (PBS). Fixation was followed by a 5-minute PBS rinse, 10-minutes staining with 2 µg/ml DAPI (4,6-diamidino-2-phenylindole; Boehringer, Mannheim) in 2× SSC (0.3 M NaCl, 0.03 M sodium citrate) and mounting in anti-fade medium (DABCO, Sigma), to count the number of nuclei/cyst. Nuclear numbers from a minimum of 100 cysts of each genotype were compared statistically using a χ^2-test.

For immunofluorescence analyses, slides of gently squashed, fixed testis were prepared. For lamin, α-tubulin, Spd2 or γ-tubulin immunostaining, testes were fixed with cold methanol for 7 minutes and permeabilized in 1× PBS containing 0.1% Tween 20 for 10 minutes. The best fixation procedure for immunostaining with anti-H3 phosphorylated at Ser10 was 3.7% paraformaldehyde in 1× PBS, followed by treatment with 45% acetic acid for 30 seconds and the squashing in 60% acetic acid as described by Giansanti et al. (Giansanti et al., 1999). Preparation of meiotic chromosomes from adult testes was performed by fixing with 45% acetic acid for 1 minute, and gently squashing under a coverslip, followed by freezing in liquid nitrogen. In all testis preparations, slides were incubated in a moist chamber for 1 hour at room temperature with the following antibody dilutions in 1× PBS: 1:100 mouse anti-LaminDm0 monoclonal (isolated by P. A. Fisher and obtained from Developmental Studies Hybridoma Bank, Iowa City, IA), 1:50 mouse anti-α-tubulin monoclonal (Sigma-Aldrich, St Louis, MO), 1:80 rabbit anti-DSpd2 [kindly provided by S. Bonaccorsi, University of Roma 'Sapienza' (Giansanti et al., 2008)], 1:1000 GTU-88 mouse anti-γ-tubulin monoclonal (Sigma-Aldrich, St Louis, MO) and 1:100 mouse anti-H3 phosphorylated at Ser10 (provided by S. Bonaccorsi, University of Roma 'Sapienza'). To detect primary antibodies, slides were incubated for 1 hour at room temperature in a moist chamber with the secondary antibodies, either Alexa-Fluor-488-conjugated goat anti-mouse IgG or Alexa-Fluor-594-conjugated goat anti-rabbit IgG (Molecular Probes, Eugene, OR), diluted according to the supplier's instructions. To visualize actin staining by phalloidin fluorescence, tissue was squashed on slides, frozen in liquid nitrogen, dehydrated in cold ethanol for 10 minutes, fixed in 3.7% paraformaldehyde and 1× PBS for 7 minutes, rehydrated in 1× PBS, incubated with blocking solution (1× PBS containing 0.1% Tween 20 and 3% BSA) for 30 minutes, then incubated for 2 hours at 37°C with 100 nM Rhodamine–phalloidin (Cytoskeleton, Inc., Denver, CO). Nuclei were stained with DAPI as described above. Testis preparations from a minimum of 10 control and 10 mutant individuals were examined for each assay.

The distribution pattern of GFP-tagged RAE1 in wild-type male meiotic cells was analyzed in the Sb^+ male progeny of the crosses between *UAS-rae1-GFP/TM6B,Sb* individuals and *BamG4UASDicer* homozygous flies; and between *UAS-rae1-GFP/TM6B,Sb* individuals and tubulin*G4/TM6B;Sb* flies. Testis preparations from Sb^+ males were obtained as described above.

Fluorescence and phase contrast images were observed with a Zeiss Axiophot fluorescence microscope equipped with a 100-W mercury light source and filter combinations suitable for the different fluorochromes (Chroma Technology Corp., Rockingham, VT, USA). Images were captured with a CCD camera (Series 200; Photometrics, Tucson, AZ) using IPLab software (Signal Analytics Corp., Vienna, VA) and processed using Adobe Photoshop (Adobe Systems, Mountain View, CA). Confocal images were captured by Zeiss LSM710 confocal microscope.

Analysis of mitotic indices

To analyze mitotic parameters, the central nervous system of third instar larvae were dissected and prepared essentially as described by Gatti and Pimpinelli (Gatti and Pimpinelli, 1983) with DAPI staining to detect chromatin and with or without colchicine treatment as described in the results. *Ore-R* larvae were used as the control. Larvae hemizygous for *ms(2)Z5584* were selected as *Tb*+ offspring from a cross of *Rec#57 ms(2)Z5584/T(2;3)Cy; Tb* females and *Df(2R)ED3923/T(2;3)Cy Tb* males. To analyze mitotic parameters of RNA-interfered strains, larvae bearing the UAS-RNAi *rae1* in combination with the Gal4 driver *wor-Gal4* were selected. Mitotic index was defined as the number of mitotic cells per optical field. Among the mitotic cells, we also classified phases as prophase/metaphase and anaphase. The optical field was the circular area defined by a 100× Zeiss objective/1.30 Plan-NEOFLUAR, using 10× oculars and the Optovar set at 1.25. Every field occupied by brain tissue on the slide was scored and at least three slides were examined for each genotype. Frequencies of mitotic figures for mutant and control genotypes were compared statistically using χ^2-test.

Sequence identification of the *ms(2)Z5584* mutation

To identify the *ms(2)Z5584* molecular lesion, genomic DNA was extracted from 30 adult males, and polymerase chain reaction (PCR) and primers (supplementary material Table S1) were used to amplify coding regions and 5′ upstream and 3′ downstream regions of specific genes (*CG30284*, *rae1*, *CG15676* and *NC2alpha*). PCR fragments were sequenced by Eurofins MWG Operon Facility (Germany) and sequences from the *ms(2)Z5584* chromosome were compared to those we obtained from control strains [*ms(2)Z3162* and *ms(2)Z1395* from the Zuker Collection for *cn bw* sequences and OreR for wild type] and to the *y; cn bw sp* stain, available from the Drosophila Genome Project (Release 5.3, http://flybase.org). The WD40-repeats of the predicted RAE1 protein were identified by SMART (Simple Modular Architecture Research Tool) motif analysis tool (http://smart.embl-heidelberg.de). The predicted RAE1 protein sequences were aligned using CLUSTALW (1.81) (http://www.genome.jp/tools/clustalw) and the following sequences for *Drosophila melanogaster* (no. AAF46745), *Mus musculus* (no. AAH59051), *Homo sapiens* (no. AAC28126), *Caenorhabditis elegans* (no. Q93454), *Schizosaccharomyces pombe* (no. CAA16856) and *Saccharomyces cerevisiae* (no. AAB64662).

ms(2)Z5584 mutant phenotype rescue by *rae1* transgene

Transgenic males homozygous for the *ms(2)Z5584* mutation and containing a third chromosome harboring both *tubulin-G4* and UAS-*GFP-rae1* were obtained (supplementary material Fig. S2). Fertility of these males were tested in matings to virgin *y w* females. These males were also used for cytological studies to compare features of spermatogenesis with those of wild-type and *ms(2)Z5584* mutant males and to monitor localization of GFP–Rae1 protein. In total, we tested 17 $rae1^{Z5584}$ homozygous males for fertility, half of which, in theory, should have been transgenic (supplementary material Fig. S2). None of these males proved fertile. Eight of these males were investigated at confocal microscope for the cytological phenotype and two of them were GFP positive.

Acknowledgements

We are deeply indebted to Chris Doe, University of Oregon, the laboratory of Margaret Fuller, Stanford University, and Chunlai Wu, Louisiana State University, for generously providing fly strains. We thank Maurizio Gatti, Silvia Bonaccorsi (University Sapienza, Rome) and members of their laboratories for valuable discussions and Luca Proietti De Santis (University of Tuscia) for his valuable advice on confocal microscopy. Confocal analysis was performed at the Major Research Equipment Center (CGA) of the University of Tuscia.

Author contributions

S.V. carried out the genetic characterization of *ms(2)Z5584* mutation. S.V. and S.B. carried out the cytological characterization of meiotic defects of *ms(2)Z5584* mutation. F.F. carried out the localization and function of a GFP–Rae1 fusion protein in the male germline. S.V., G.P. and B.T.W. wrote the paper. G.P. and B.T.W. conceived and designed the experiments.

Funding

This work was supported by the University of Tuscia ("Ricerca di Ateneo" grant to G.P.).

Supplementary material available online at
http://jcs.biologists.org/lookup/suppl/doi:10.1242/jcs.111328/-/DC1

References

Alphey, L., Jimenez, J., White-Cooper, H., Dawson, I., Nurse, P. and Glover, D. M. (1992). twine, a cdc25 homolog that functions in the male and female germline of Drosophila. *Cell* **69**, 977-988.

Anderson, M. A., Jodoin, J. N., Lee, E., Hales, K. G., Hays, T. S. and Lee, L. A. (2009). Asunder is a critical regulator of dynein-dynactin localization during Drosophila spermatogenesis. *Mol. Biol. Cell* **20**, 2709-2721.

Babu, J. R., Jeganathan, K. B., Baker, D. J., Wu, X., Kang-Decker, N. and van Deursen, J. M. (2003). Rae1 is an essential mitotic checkpoint regulator that cooperates with Bub3 to prevent chromosome missegregation. *J. Cell Biol.* **160**, 341-353.

Basu, J., Bousbaa, H., Logarinho, E., Li, Z., Williams, B. C., Lopes, C., Sunkel, C. E. and Goldberg, M. L. (1999). Mutations in the essential spindle checkpoint gene bub1 cause chromosome missegregation and fail to block apoptosis in Drosophila. *J. Cell Biol.* **146**, 13-28.

Bharathi, A., Ghosh, A., Whalen, W. A., Yoon, J. H., Pu, R., Dasso, M. and Dhar, R. (1997). The human RAE1 gene is a functional homologue of Schizosaccharomyces pombe rae1 gene involved in nuclear export of Poly(A)$^+$ RNA. *Gene* **198**, 251-258.

Blower, M. D., Nachury, M., Heald, R. and Weis, K. (2005). A Rae1-containing ribonucleoprotein complex is required for mitotic spindle assembly. *Cell* **121**, 223-234.

Brown, J. A., Bharathi, A., Ghosh, A., Whalen, W., Fitzgerald, E. and Dhar, R. (1995). A mutation in the Schizosaccharomyces pombe rae1 gene causes defects in poly(A)$^+$ RNA export and in the cytoskeleton. *J. Biol. Chem.* **270**, 7411-7419.

Bucciarelli, E., Giansanti, M. G., Bonaccorsi, S. and Gatti, M. (2003). Spindle assembly and cytokinesis in the absence of chromosomes during Drosophila male meiosis. *J. Cell Biol.* **160**, 993-999.

Cabernard, C. and Doe, C. Q. (2009). Apical/basal spindle orientation is required for neuroblast homeostasis and neuronal differentiation in Drosophila. *Dev. Cell* **17**, 134-141.

Cenci, G., Bonaccorsi, S., Pisano, C., Verni, F. and Gatti, M. (1994). Chromatin and microtubule organization during premeiotic, meiotic and early postmeiotic stages of Drosophila melanogaster spermatogenesis. *J. Cell Sci.* **107**, 3521-3534.

Chintapalli, V. R., Wang, J. and Dow, J. A. (2007). Using FlyAtlas to identify better Drosophila melanogaster models of human disease. *Nat. Genet.* **39**, 715-720.

Courtot, C., Fankhauser, C., Simanis, V. and Lehner, C. F. (1992). The Drosophila cdc25 homolog twine is required for meiosis. *Development* **116**, 405-416.

Dietzl, G., Chen, D., Schnorrer, F., Su, K. C., Barinova, Y., Fellner, M., Gasser, B., Kinsey, K., Oppel, S., Scheiblauer, S. et al. (2007). A genome-wide transgenic RNAi library for conditional gene inactivation in Drosophila. *Nature* **448**, 151-156.

Fuller, M. T. (1993). Spermatogenesis. In *The Development of Drosophila melanogaster* (ed. M. Bate and A. Martinez Arias), pp. 71-147. Cold Spring Harbor, NY: Cold Spring Harbor Laboratory Press.

Gatti, M. and Pimpinelli, S. (1983). Cytological and genetics analysis of the Y chromosome of Drosophila melanogaster. I. Organization of the fertility factors. *Chromosoma* **88**, 349-373.

Giansanti, M. G., Bonaccorsi, S. and Gatti, M. (1999). The role of anillin in meiotic cytokinesis of Drosophila males. *J. Cell Sci.* **112**, 2323-2334.

Giansanti, M. G., Bucciarelli, E., Bonaccorsi, S. and Gatti, M. (2008). Drosophila SPD-2 is an essential centriole component required for PCM recruitment and astral-microtubule nucleation. *Curr. Biol.* **18**, 303-309.

Hartl, T. A., Sweeney, S. J., Knepler, P. J. and Bosco, G. (2008). Condensin II resolves chromosomal associations to enable anaphase I segregation in Drosophila male meiosis. *PLoS Genet.* **4**, e1000228.

Ichihara, K., Shimizu, H., Taguchi, O., Yamaguchi, M. and Inoue, Y. H. (2007). A Drosophila orthologue of larp protein family is required for multiple processes in male meiosis. *Cell Struct. Funct.* **32**, 89-100.

Jeganathan, K. B., Baker, D. J. and van Deursen, J. M. (2006). Securin associates with APCCdh1 in prometaphase but its destruction is delayed by Rae1 and Nup98 until the metaphase/anaphase transition. *Cell Cycle* **5**, 366-370.

Koundakjian, E. J., Cowan, D. M., Hardy, R. W. and Becker, A. H. (2004). The Zuker collection: a resource for the analysis of autosomal gene function in Drosophila melanogaster. *Genetics* **167**, 203-206.

Lee, J. Y., Lee, H. S., Wi, S. J., Park, K. Y., Schmit, A. C. and Pai, H. S. (2009). Dual functions of Nicotiana benthamiana Rae1 in interphase and mitosis. *Plant J.* **59**, 278-291.

Maines, J. Z. and Wasserman, S. A. (1999). Post-transcriptional regulation of the meiotic Cdc25 protein Twine by the Dazl orthologue Boule. *Nat. Cell Biol.* **1**, 171-174.

Matsui, M., Sharma, K. C., Cooke, C., Wakimoto, B. T., Rasool, M., Hayworth, M., Hylton, C. A. and Tomkiel, J. E. (2011). Nuclear structure and chromosome segregation in Drosophila male meiosis depend on the ubiquitin ligase dTopors. *Genetics* **189**, 779-793.

McQuilton, P., St Pierre, S. E., Thurmond, J.; FlyBase Consortium (2012). FlyBase 101—the basics of navigating FlyBase. *Nucleic Acids Res.* **40**, D706-D714.

Murphy, R., Watkins, J. L. and Wente, S. R. (1996). GLE2, a Saccharomyces cerevisiae homologue of the Schizosaccharomyces pombe export factor RAE1, is required for nuclear pore complex structure and function. *Mol. Biol. Cell* **7**, 1921-1937.

Nakano, H., Funasaka, T., Hashizume, C. and Wong, R. W. (2010). Nucleoporin translocated promoter region (Tpr) associates with dynein complex, preventing chromosome lagging formation during mitosis. *J. Biol. Chem.* **285**, 10841-10849.

Neer, E. J., Schmidt, C. J., Nambudripad, R. and Smith, T. F. (1994). The ancient regulatory-protein family of WD-repeat proteins. *Nature* **371**, 297-300.

Pritchard, C. E., Fornerod, M., Kasper, L. H. and van Deursen, J. M. (1999). RAE1 is a shuttling mRNA export factor that binds to a GLEBS-like NUP98 motif at the nuclear pore complex through multiple domains. *J. Cell Biol.* **145**, 237-254.

Rebollo, E., Llamazares, S., Reina, J. and Gonzalez, C. (2004). Contribution of noncentrosomal microtubules to spindle assembly in Drosophila spermatocytes. *PLoS Biol.* **2**, E8.

Reddy, D. M., Aspatwar, A., Dholakia, B. B. and Gupta, V. S. (2008). Evolutionary analysis of WD40 super family proteins involved in spindle checkpoint and RNA export: molecular evolution of spindle checkpoint. *Bioinformation* **2**, 461-468.

Sabri, N. and Visa, N. (2000). The Ct-RAE1 protein interacts with Balbiani ring RNP particles at the nuclear pore. *RNA* **6**, 1597-1609.

Sigrist, S., Ried, G. and Lehner, C. F. (1995). Dmcdc2 kinase is required for both meiotic divisions during Drosophila spermatogenesis and is activated by the Twine/cdc25 phosphatase. *Mech. Dev.* **53**, 247-260.

Sitterlin, D. (2004). Characterization of the Drosophila Rae1 protein as a G1 phase regulator of the cell cycle. *Gene* **326**, 107-116.

Tian, X., Li, J., Valakh, V., DiAntonio, A. and Wu, C. (2011). Drosophila Rae1 controls the abundance of the ubiquitin ligase Highwire in post-mitotic neurons. *Nat. Neurosci.* **14**, 1267-1275.

Wakimoto, B. T., Lindsley, D. L. and Herrera, C. (2004). Toward a comprehensive genetic analysis of male fertility in Drosophila melanogaster. *Genetics* **167**, 207-216.

Wang, X., Babu, J. R., Harden, J. M., Jablonski, S. A., Gazi, M. H., Lingle, W. L., de Groen, P. C., Yen, T. J. and van Deursen, J. M. (2001). The mitotic checkpoint protein hBUB3 and the mRNA export factor hRAE1 interact with GLE2p-binding sequence (GLEBS)-containing proteins. *J. Biol. Chem.* **276**, 26559-26567.

Whalen, W. A., Bharathi, A., Danielewicz, D. and Dhar, R. (1997). Advancement through mitosis requires rae1 gene function in fission yeast. *Yeast* **13**, 1167-1179.

White-Cooper, H. (2010). Molecular mechanisms of gene regulation during Drosophila spermatogenesis. *Reproduction* **139**, 11-21.

White-Cooper, H., Alphey, L. and Glover, D. M. (1993). The cdc25 homologue twine is required for only some aspects of the entry into meiosis in Drosophila. *J. Cell Sci.* **106**, 1035-1044.

Wong, R. W. (2010). Interaction between Rae1 and cohesin subunit SMC1 is required for proper spindle formation. *Cell Cycle* **9**, 198-200.

Wong, R. W., Blobel, G. and Coutavas, E. (2006). Rae1 interaction with NuMA is required for bipolar spindle formation. *Proc. Natl. Acad. Sci. USA* **103**, 19783-19787.